On Defining a Simple Empirical Relationship to Predict the Pore Size of Mesoporous Silicas Prepared from PEO-*b*-PS Diblock Copolymers

Emily Bloch,[†] Philip L. Llewellyn,[†] Trang Phan,[‡] Denis Bertin,[‡] and Virginie Hornebecq[†,*]

Equipe Matériaux Divisés: Réactivité, Elaboration and Equipe Chimie Radicalaire, Organique et Polymères de Spécialité, Laboratoire Chimie Provence, Universités d'Aix-Marseille I, II, et III-CNRS UMR 6264, Centre St Jérôme, 13397 Marseille Cedex 20, France

Received April 23, 2008. Revised Manuscript Received November 10, 2008

Mesoporous silicas with large and accessible pores have been successfully synthesized using laboratory-made poly(ethylene oxide)-*b*-polystyrene (PEO-*b*-PS) copolymers as templates. The PEO-*b*-PS copolymers were synthesized using living/controlled radical polymerization. The porous structure (mesopore size, size distribution, and microporous volume) was characterized using small-angle X-ray scattering, electron transmission microscopy, and nitrogen sorption measurements. In this study, we have investigated the dependence of the mesoporosity on both the PS and PEO blocks length using two series of PEO-*b*-PS copolymers with a constant degree of polymerization of the PEO block for each series ($N_{PEO} = 114$ and $N_{PEO} = 232$). It was found that the mesopore size increases and the microporous volume decreases as the PS block length (N_{PS}) increases. The PEO block participates to both the micropore and mesopore formation. By fitting these experimental data, a simple empirical relationship between the pore radius and the length of the both PS block (N_{PS}) and PEO block (N_{PEO}) is found R_P (nm) $= 0.36.N_{PEO}^{0.19}N_{PS}^{0.5}$. This relationship is in agreement for both low- and high-molecular-weight copolymers and can be easily be used to fine-tune the mesopore size of silica materials, in a large range (from 4 to 22 nm), when using PEO-*b*-PS copolymers as templates. Furthermore, the influence of the synthesis temperature (between 25 and 60 °C) on the porous structure was also investigated and it was found that by increasing the synthesis temperature, the mesopore diameters remain relatively constant; however, the pore entrances increase in size, leading to more open pore structures.

1. Introduction

The development of mesoporous silica presenting large and accessible pores has received much attention because of their potential applications involving large molecules including enzymes and proteins.[1] Other potential applications have been suggested in adsorption, separation, catalysis, as nanodevices, or as photonic waveguides.[2−6] Numerous studies have focused on the surfactant "structure directing agent" (or SDA) itself in order to obtain such mesoporous silicas having the required pore size and accessibility. In these cases, diblock and triblock copolymers are often used as SDAs. However, although well-structured materials have been obtained, very few studies have been devoted to understanding the role of each block on the inorganic materials thus obtained. Such work is essential for those looking to prepare mesoporous silica materials for a specific application where a well controlled pore size and geometry are required. The present study is aimed at filling this gap in the case where amphiphilic PEO-*b*-PS diblock copolymers SDAs are used.

Amphiphilic block copolymers belong to an important family of surfactants and have been increasingly used to organize mesostructured metal oxides.[7] They also are used for drug delivery[8] and nanostructure fabrication.[9] They have the advantage that their ordering properties can be continuously tuned by adjusting the solvent composition,[10] molecular weight,[11] or polymer architecture.[12,13] These properties can be used in many applications.[14] In the context of mesostructured oxides, many studies have reported the use of poly(ethylene oxide)-*b*-poly(propylene oxide)-*b*-poly(ethylene oxide) (PEO-*b*-PPO-*b*-PEO) triblock copolymers as templates in the synthesis of mesoporous silica structures.[11,15−18] PEO-

* To whom correspondence should be addressed. E-mail: virginie.hornebecq@univ-provence.fr. Phone: 33 491 637120. Fax: 33 491 637111.
[†] Equipe Matériaux Divisés: Réactivité, Elaboration.
[‡] Equipe Chimie Radicalaire, Organique et Polymères de Spécialité.

(1) Hartmann, M. *Chem. Mater.* **2005**, *17*, 4577.
(2) Beck, J. S.; Vartuli, J. C. *Curr. Opin. Solid State Mater. Sci.* **1996**, *1*, 76.
(3) Corma, A. *Chem. Rev.* **1997**, *97*, 2373.
(4) Diaz, J. F.; Balkus, K. J. *J. Mol. Catal. B: Enzym.* **1996**, *2*, 115.
(5) Han, Y. J.; Kim, J. M.; Stucky, G. D. *Chem. Mater.* **2000**, *12*, 2068.
(6) Moller, K.; Bein, T. *Chem. Mater.* **1998**, *10*, 2950.
(7) Soler-Illia, G.; Crepaldi, E. L.; Grosso, D.; Sanchez, C. *Curr. Opin. Colloid Interface Sci.* **2003**, *8*, 109.
(8) Torchilin, V. P. *Expert Opin. Ther. Pat.* **2005**, *15*, 63.
(9) Hamley, I. W. *Nanotechnology* **2003**, *14*, R39.
(10) Kleitz, F.; Kim, T. W.; Ryoo, R. *Langmuir* **2006**, *22*, 440.
(11) Zhao, D. Y.; Feng, J. L.; Huo, Q. S.; Melosh, N.; Fredrickson, G. H.; Chmelka, B. F.; Stucky, G. D. *Science* **1998**, *279*, 548.
(12) Soler-Illia, G. J. D.; Sanchez, C.; Lebeau, B.; Patarin, J. *Chem. Rev.* **2002**, *102*, 4093.
(13) Ciesla, U.; Schuth, F. *Microporous Mesoporous Mater.* **1999**, *27*, 131.
(14) Darling, S. B. *Prog. Polym. Sci.* **2007**, *32*, 1152.
(15) Imperor-Clerc, M.; Davidson, P.; Davidson, A. *J. Am. Chem. Soc.* **2000**, *122*, 11925.
(16) Kleitz, F.; Choi, S. H.; Ryoo, R. *Chem. Comm.* **2003**, 2136.
(17) Kleitz, F.; Liu, D. N.; Anilkumar, G. M.; Park, I. S.; Solovyov, L. A.; Shmakov, A. N.; Ryoo, R. *J. Phys. Chem. B* **2003**, *107*, 14296.

10.1021/cm801978w CCC: $40.75
Published on Web 12/11/2008

b-PPO-*b*-PEO triblock copolymers are commercially available with trade name Pluronic. However, because of the limitation of their molecular weight composition, templated mesoporous silicas with mesoscopic order have been limited to pore sizes of around 10−12 nm. Other synthesis routes have been used to extend this range of pore size. The first is the use of swelling agents such as trimethylbenzene, decane, or *n*-butanol, which leads to the formation of mesocellular foams whose pore sizes vary between 20 and 40 nm.[19] However, this method involves many complicated synthesis steps that limit their use. Another method to expand the pore size has been to synthesize higher-molecular-weight amphiphilic copolymers than those commercially available and use these as SDAs. Therefore, high-molecular-weight copolymers with long hydrophobic segments can become good candidates to template large pore mesoporous silicas.[20,21] Templin et al.[22] first used poly(isoprene)-*b*-poly(ethylene oxide) block copolymers (PI-*b*-PEO), synthesized via living anionic polymerization, to prepare mesostructured aluminosilicate-polymer composites with ordered length scales up to 40 nm. Göltner et al.[23] used polybutadiene-*b*-poly(ethylene oxide) PB-*b*-PEO copolymers as templates. They obtained unconventional pore morphologies including branched lamellar phases and bicontinuous sponge-like structures with diameters less than 20 nm.

Several studies have been devoted to the use of high molecular weight polystyrene-*b*-poly(ethylene oxide) (PS-*b*-PEO) as SDAs. Yu et al.[21] and Smarsly et al.[24] prepared PS-*b*-PEO copolymers by the sequential anionic polymerization of the styrene monomer followed by the ethylene oxide monomer. They were thus able to synthesize two ordered mesoporous silica (with PS_{215}-*b*-PEO_{100} and PS_{35}-*b*-PEO_{109}) thin films with pore diameters of 18 and 5 nm, respectively. Recently, Deng et al.[25] synthesized highly ordered mesoporous carbons and silicas with ultralarge pores (∼30 nm) by one laboratory-made PEO-*b*-PS SDA, which was prepared via atom transfer radical polymerization. However, the sample required a supplementary hydrothermal recrystallization step at 100 °C for 3 days prior to calcination in order to be able to access the porosity.

Several studies have attempted to understand the relationship between the block copolymer and the subsequent silica structure obtained. Göltner et al.,[26,27] using low molecular weight commercial PS-*b*-PEO copolymers as templates, studied the influence of the hydrophilic PEO block on the porous structure. In order to predict the mesopore size, Smarsly et al.[28] prepared porous silica materials via sol−gel nanocasting of low molecular weight nonionic surfactants (*n*-alkyl-poly(ethylene oxide) amphiphilic "C_xE_y"). They found that the mesopore size depends on the length of the alkyl chain and on the length of the PEO block, and a fairly complicated empirical dependence was found. This empirical relationship is explained by a three phases model and allows an explanation of both the influence the alkyl and poly(ethylene oxide) chains on the micropore and mesopore diameters up to 3 nm. These studies thus highlight an interesting strategy to prepare mesopores and show the first attempts to understand the role of the hydrophobic and/or the hydrophilic block on the porous structure.

In this paper, we report a rational sol−gel synthesis of mesoporous silica with large diameter between 4 and 22 nm and accessible pores using laboratory made PEO-*b*-PS diblock copolymers as SDAs. The well-defined PEO-*b*-PS diblock copolymers were synthesized using nitroxide-mediated polymerization.[29−31] The effects of the polystyrene (PS) and the poly(ethylene oxide) (PEO) block lengths on the subsequently synthesized mesoporous silica are investigated. To understand the role of each block on the porous network (size and organization), silica matrices were characterized using small-angle X-ray scattering (SAXS), transmission electron microscopy (TEM) and nitrogen sorption measurements at 77 K. These results allow, for the first time, a simple empirical mathematical relationship to be obtained between the pore radii and the degree of polymerization of both the PS and PEO blocks. Further to this, the influence of the synthesis temperature (from 25 to 60 °C) on the porous structure was also investigated.

2. Experimental Section

2.1. Reagents. Monomethoxy poly(ethylene oxide) [$H_3C(OCH_2CH_2)_nOH$], styrene (99%), acryloyl chloride (96%) and triethylamine (99%) were all purchased from Aldrich Chemical Co. and used as supplied. The SG_1-based alkoxyamine derived from methacrylic-acid, also called MAMA-SG_1 (Acid 2-methyl-2-[N-*tert*-butyl-N-(1-diethoxyphosphoryl-2,2-dimethyl propyl)aminoxy] propanoic) or BlocBuilder was kindly supplied by ARKEMA. All solvents and products were used without any further purification.

For the synthesis of the silica matrix, hydrochloric acid (HCl) with a pH of 2 was prepared by adding the appropriate amount of HCl (32 wt %) to distilled water. The tetramethyl orthosilicate (98%) ($Si(CH_3O)_4$) (TMOS) was used as silica source (Aldrich).

2.2. Synthesis of Diblock Copolymers. The PEO-*b*-PS copolymers were obtained by using living/controlled radical polymerization method. The polystyrene block was synthesized by nitroxide mediated polymerization (NMP) from poly(ethylene oxide) mac-

(18) Zhao, D. Y.; Huo, Q. S.; Feng, J. L.; Chmelka, B. F.; Stucky, G. D. *J. Am. Chem. Soc.* **1998**, *120*, 6024.
(19) Lettow, J. S.; Han, Y. J.; Schmidt-Winkel, P.; Yang, P. D.; Zhao, D. Y.; Stucky, G. D.; Ying, J. Y. *Langmuir* **2000**, *16*, 8291.
(20) Thomas, A.; Schlaad, H.; Smarsly, B.; Antonietti, M. *Langmuir* **2003**, *19*, 4455.
(21) Yu, K.; Hurd, A. J.; Eisenberg, A.; Brinker, C. J. *Langmuir* **2001**, *17*, 7961.
(22) Templin, M.; Franck, A.; DuChesne, A.; Leist, H.; Zhang, Y. M.; Ulrich, R.; Schadler, V.; Wiesner, U. *Science* **1997**, *278*, 1795.
(23) Goltner, C. G.; Berton, B.; Kramer, E.; Antonietti, M. *Adv. Mater.* **1999**, *11*, 395.
(24) Smarsly, B.; Xomeritakis, G.; Yu, K.; Liu, N. G.; Fan, H. Y.; Assink, R. A.; Drewien, C. A.; Ruland, W.; Brinker, C. J. *Langmuir* **2003**, *19*, 7295.
(25) Deng, Y. H.; Yu, T.; Wan, Y.; Shi, Y. F.; Meng, Y.; Gu, D.; Zhang, L. J.; Huang, Y.; Liu, C.; Wu, X. J.; Zhao, D. Y. *J. Am. Chem. Soc.* **2007**, *129*, 1690.
(26) Goltner, C. G.; Smarsly, B.; Berton, B.; Antonietti, M. *Chem. Mater.* **2001**, *13*, 1617.
(27) Goltner, C. G.; Henke, S.; Weissenberger, M. C.; Antonietti, M. *Angew. Chem., Int. Ed.* **1998**, *37*, 613.
(28) Smarsly, B.; Polarz, S.; Antonietti, M. *J. Phys. Chem. B* **2001**, *105*, 10473.
(29) Bertin, D.; Chauvin, F.; Marque, S.; Tordo, P. *Macromolecules* **2002**, *35*, 3790.
(30) Dufils, P. E.; Petit, C.; Gigmes, D.; Beaudouin, E.; Marque, S.; Bertin, D.; Tordo, P.; Guerret, O.; Couturier, J. L. *ACS Polym. Prepr.* **2004**, *227*, U401.
(31) Hua, F. J.; Yang, Y. L. *Polymer* **2001**, *42*, 1361.

Table 1. Characteristics of the PEO-*b*-PS Copolymers and the Corresponding Silica Samples

silica sample	copolymer sample	M_n (PS) (g mol^{-1})	M_n (PEO) (g.mol^{-1})	N_{PS}	N_{PEO}
SEO-1	$PEO_{114}-PS_{19}$	2000	5000	19	114
SEO-2	$PEO_{114}-PS_{48}$	5000	5000	48	114
SEO-3	$PEO_{114}-PS_{115}$	12 000	5000	115	114
SEO-4	$PEO_{232}-PS_{28}$	3000	10 000	28	232
SEO-5	$PEO_{232}-PS_{72}$	7500	10 000	72	232
SEO-6	$PEO_{232}-PS_{96}$	10 000	10 000	96	232
SEO-7	$PEO_{232}-PS_{115}$	12 000	10 000	115	232

roalkoxyamine. The synthetic procedure of PEO-*b*-PS diblock copolymers is similar to that used for synthesizing PS-*b*-PEO-*b*-PS triblock copolymers. Experimental details of the synthesis and characterization of PEO-macroalkoxyamine as well as PS-*b*-PEO-*b*-PS were described previously.[32] As a reminder, the synthetic procedure of PEO-*b*-PS involves three steps. The first one is the esterification of the hydroxyl-terminated PEO with an acryloyl chloride to form an acrylate of poly(ethylene oxide). The second step is the intermolecular addition between the acrylate of poly(ethylene oxide) and the MAMA-SG_1 to product the PEO-macroalkoxyamine. The last step is the use of the latter to initiate the polymerization of styrene. The successful preparation of PEO-acrylate, PEO-macroalkoxyamine, and PEO-*b*-PS was confirmed by ^{1}H and ^{31}P NMR spectroscopy. These analyses were preformed in $CDCl_3$ containing 0.1% TMS (tetramethylsilane) as an internal reference on a BRUKER Avance DPX-300 spectrometer. All PEO_x-*b*-PS_y diblock copolymers used for the synthesis of mesoporous silicas are listed in Table 1.

2.3. Synthesis of Mesoporous Silica. PEO_x-*b*-PS_y diblock copolymers are insoluble in water or ethanol because of the high molecular weight of the PS block, so the copolymer was dissolved in tetrahydrofuran (THF) and stirred at room temperature. After solubilization of the copolymer, hydrochloric acid (HCl) 0.01 M and tetramethyl orthosilicate (TMOS) were added. The mass ratio was 1:1:2:7 [copolymer:HCl:TMOS:THF]. Stirring was continued until gelification at a fixed synthesis temperature (25, 45, or 60 °C). Then, the as-formed clear gel was aged for 1 week at room temperature. The organic templates were removed by calcination at 650 °C in air for 6 h. The silica samples are named SEO-Z depending of the PEO_x-*b*-PS_y diblock copolymers used as template. When the sample is synthesized at 45 or 60 °C, the sample is named SEO-Z-45 or SEO-Z-60. The characteristics of silica samples synthesized at 25 °C are reported in Table 1.

2.4. Characterization of Mesoporous Silicas. Small-angle X-ray scattering experiments were performed at the bending magnet beamline BM02 (D2AM) of the European Synchrotron Radiation facility (Grenoble, France) with the energy set at 11 keV. This beamline was already described in detail.[33] The data was acquired using a CCD Peltier-cooled camera (SCX90−1300, from Princeton Instruments Inc., New Jersey) with 1340 × 1300 pixels. Data preprocessing (dark current subtraction, flat field correction, radial regrouping and normalization) was performed using the bm2img software developed at the beamline. For the transmission electron microscopy, calcined samples were dispersed in methanol (99.9 vol. %), and the suspension was subsequently dropped onto a carbon microgrid. The transmission electron microscopy mesostructural images of silicas matrices were recorded on a JEOL JEM 2010F transmission electron microscope (TEM). The N_2 adsorption−desorption isotherms were obtained at 77 K on a Micrometrics ASAP 2010. The specific surface area was determined with the Brunauer, Emmett, and Teller (BET) method and the pore size distribution was calculated from the adsorption isotherms using the Barrett−Joyner−Halenda (BJH) method.[34] Prior to adsorption, the samples were outgassed at 393 K overnight under a vaccum pressure of 2 × 10^{-3} mbar.

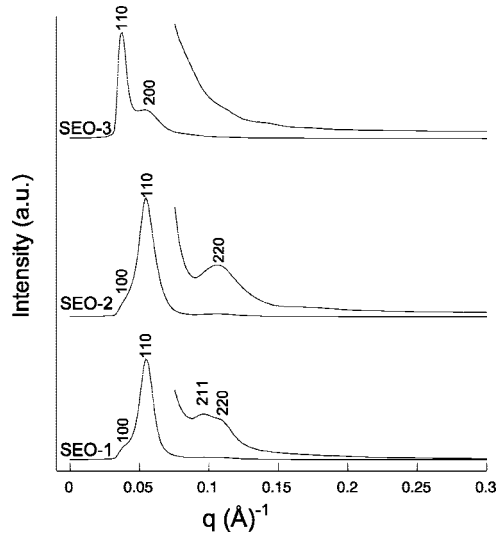

Figure 1. XRD patterns of calcined mesoporous silicas with $N_{PEO} = 114$.

3. Results and Discussions

3.1. Influence of the Degree of Polymerization of the PS and PEO Blocks on the Resulting Porous Structure Prepared at 25 °C. To study the influence of the degree of polymerization of both the PS (N_{PS}) and the PEO (N_{PEO}) blocks on the porous structure, we prepared two series of silica matrices at 25 °C using PEO-*b*-PS copolymers with a N_{PEO} block constant equal to 114 or to 232. In this manner, in each series, we will focus on the influence of N_{PS}, whereas comparing the two series permits us to study the influence of N_{PEO}.

3.1.1. Study of the Organization of the Porous Structure. X-ray diffraction (XRD) patterns of silicas matrices (SEO-1, -2, -3 samples) prepared with $N_{PEO} = 114$ copolymers are presented in Figure 1. For the SEO-1 and SEO-2 samples, the XRD patterns are similar and show two or three resolved diffraction peaks and one shoulder at very low q value that can be indexed to the (100), (110), (211,) and (220) reflections of the primitive $Pm\bar{3}m$ cubic structure. The unit-cell parameter, a_{calc}, calculated from the (110) reflection is 16.2 and 16.4 nm for SEO-1 and SEO-2 samples, respectively. This $Pm\bar{3}m$ space group has previously been reported for SBA-11 materials synthesized in the presence of $C_{16}EO_{10}$ (BRIJ 56) surfactants.[18]

TEM images of these mesoporous silicas reveal a homogeneous pore structure and an organization of pores can be observed (images a and b in Figure 2). The cell parameter estimated from TEM images is about 15 nm for SEO-1 and

(32) Bloch, E.; Phan, T.; Bertin, D.; Llewellyn, P.; Hornebecq, V. *Microporous Mesoporous Mater.* **2008**, *112*, 612.
(33) Simon, J. P.; Arnaud, S.; Bley, F.; Berar, J. F.; Caillot, B.; Comparat, V.; Geissler, E.; de Geyer, A.; Jeantey, P.; Livet, F.; Okuda, H. *J. Appl. Crystallogr.* **1997**, *30*, 900.
(34) Rouquerol, F.; Rouquerol, J.; Sing, K. S. W., *Adsorption by Powders and Porous Solids: Principles, Methodology and Applications*; Academic Press: London, 1999.

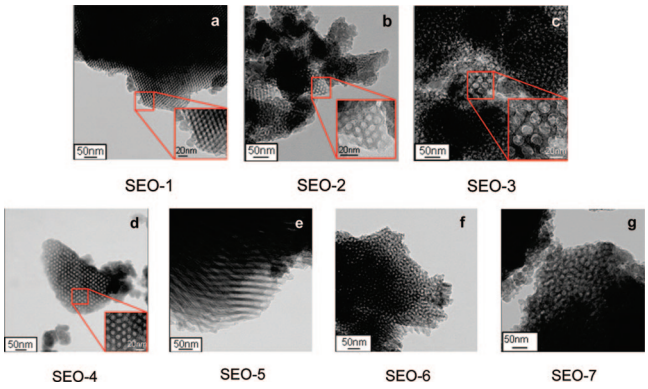

Figure 2. TEM images of calcined mesoporous silicas prepared using PEO-*b*-PS copolymers with $N_{PEO} = 114$ (a−c) and $N_{PEO} = 232$ (d−g).

SEO-2 samples consistent with the value determined using X-ray diffraction. For the SEO-3 sample, the XRD pattern exhibits a less-ordered structure and some differences compared to the two others were noted: the intensity of the diffraction peak (110) increases, whereas the intensity of the second one decreases and the two peaks of (211) and (220) reflections according to the $Pm\bar{3}m$ symmetry are absent. This suggests some changes in the mesostructure for this sample. Furthermore, the cell parameter estimated from TEM images (Figure 2c) is about 26 nm. This value is no longer consistent with the $Pm\bar{3}m$ symmetry. Because of the limited number of diffraction peaks, it is difficult to index them even if they could be consistent with the $Im\bar{3}m$ symmetry ($a_{calc} \approx 24$ nm).The indexation of peaks using this space group is reported in Figure 2c. In light of these results, it seems that there is a change in the symmetry of the mesostructure with an increasing degree of polymerization of the PS block.

Concerning the second series of mesoporous silicas prepared using PEO-*b*-PS ($N_{PEO} = 232$) copolymers as templates, X-ray diffraction results are difficult (not shown) to interpret. Indeed, only the first sample of the series (SEO-4) exhibits two diffractions peaks that can be indexed to the (100) and (200) reflections of the primitive $Pm\bar{3}m$ cubic structure with a corresponding cell parameter a equal to 16 nm. TEM images of these mesoporous silicas (Figure 2d−g) reveal a homogeneous pore structure and for samples with the lowest degree of polymerization of the PS block (SEO-4 and SEO-5), an organization of pores is found. The cell parameter estimated from TEM images is about 18 nm for SEO-4, consistent with the value determined using X-ray diffraction. In the second series of samples (from SEO-4 to SEO-7), it seems that the increase in the degree of polymerization of the PS block leads to a loss of pore organization.

3.1.2. Evolution of the Mesopore Diameter. A first characterization of the mesopore size has been obtained from the analysis of the precedent TEM pictures. For each sample, the determined pore diameter is reported in Table 2. A general trend is found for both series: when N_{PS} increases, the pore diameter increases.

To confirm this evolution and to fully characterize the mesostructure (mean pore diameter, specific surface area, and microporous volume), we performed nitrogen sorption measurements at 77 K. The nitrogen adsorption/desorption isotherms obtained are shown in panels a and b in Figure 3. They are all characterized by an initial sharp uptake at a relative pressure below 0.05 followed by a more gradual uptake before a second sharp upswing in the curves between relative pressures of 0.65 and 0.85 depending on the sample. A final short plateau ends the adsorption branch. Such isotherms can be characterized by the IUPAC as mixed type I and type IV isotherms, which are attributed to samples containing both microporosity and rigid mesoporosity.[35] The equivalent surface areas were calculated with the BET method. The values of the BET surface area can be taken only to an estimation because of the presence of micoporosity, so the term "equivalent" BET surface area is used. These BET values are given in Table 2 along with estimations of the micropore volume determined from the t-plot method. The size of the mesopores can be estimated using the BJH method applied to the adsorption branch of the isotherms and the values obtained are again given in Table 2. There is some criticism of the use of the original BJH method, which has especially been noted with respect to the evaluation of especially mesoporous silica's in the lower range of mesopore size. This has been attributed to both the hypothesis of cylindrical pores and/or the description of the multilayer.[36,37] Several solutions have been proposed and when the latter solution[37] was tested in the present case, it did not particularly change our findings.[36,37] Further, NLDFT[38] can be used to evaluate the pore sizes but in our case, it was impossible to find appropriate kernels for the pore sizes above 10 nm. Thus, although BJH can be criticized, our pore diameter values from BJH and those determined previously from TEM analysis, as well as those obtained by NLDFT for pore sizes below 10 nm, are in fairly good agreement.

Table 2. Porous Properties of the Silica Matrices Obtained with $N_{PEO} = 114$ and $N_{PEO} = 232$

silica samples	D_{pore} (TEM) (nm)	D_{pore} $(BJH)_{ads}$ (nm)	BET area ($m^2\ g^{-1}$)	micropore volume ($cm^3\ g^{-1}$)
SEO-1	(8 ± 2)	5	573	(0.13 ± 0.01)
SEO-2	(11 ± 2)	7	421	(0.10 ± 0.01)
SEO-3	(19 ± 2)	18	239	(0.06 ± 0.01)
SEO-4	(11 ± 2)	9	437	(0.13 ± 0.01)
SEO-5	(16 ± 2)	16	300	(0.09 ± 0.01)
SEO-6	(20 ± 2)	20	280	(0.09 ± 0.01)
SEO-7	(22 ± 2)	22	293	(0.08 ± 0.01)

Turning to the desorption, most of the samples show hysteresis (images a and b in Figure 3) of similar form and end in the same relative pressure region between 0.48 and 0.5. Note that these values are above the value of $p/p^0 = 0.42$, which corresponds to the point of nitrogen meniscus instability and to a cavitation effect. Therefore, the hysteresis observed here is directly due to the pore shape, and such desorption branches are typically observed for mesopores with small entrances.[35] An estimation of these pore openings from NLDFT suggests widths of around 5 nm.

One exception can be observed for the sample SEO-1 (PEO_{114}-*b*-PS_{19}) in which the desorption occurs in two steps; the first desorption occurs at around $p/p^0 = 0.65$ with a

(35) Sing, K. S. W.; Everett, D. H.; Haul, R. A. W.; Moscou, L.; Pierotti, R. A.; Rouquerol, J.; Siemieniewska, T. *Pure Appl. Chem.* **1985**, *57*, 603.
(36) Kleitz, F.; Czuryszkiewicz, T.; Solovyov, L. A.; Linden, M. *Chem. Mater.* **2006**, *18*, 5070.
(37) Kruk, M.; Jaroniec, M.; Sayari, A. *Langmuir* **1997**, *13*, 6267.
(38) Ravikovitch, P. I.; Neimark, A. V. *J. Phys. Chem. B* **2001**, *105*, 6817.

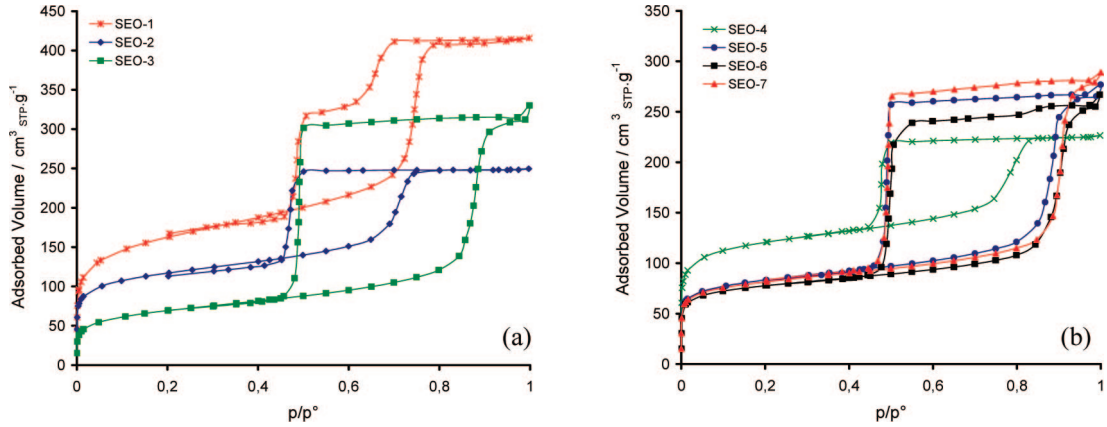

Figure 3. Nitrogen adsorption/desorption isotherms of SEO-Z samples with N_{PEO} constant. (a) $N_{PEO} = 114$ and (b) $N_{PEO} = 232$.

second one below $p/p^0 = 0.5$ as for the other samples. This desorption hysteresis suggests the presence of two types of pore openings, and an estimation of these from NLDFT suggests openings of approximately 8 and 5 nm, respectively.

These results allow one to follow the evolution the pore diameter as a function of the PS block. Concerning the evolution of the pore size, for each series (either $N_{PEO} = 114$ or $N_{PEO} = 232$), a general trend is confirmed: when N_{PS} increases the pore diameter increases.

3.1.3. Toward an Empirical Relationship for Pore Size Prediction. Above the critical micellar concentration (cmc), diblock copolymers self-assemble into micellar structures in a selective solvent. Current theories picture a block copolymer micelle in terms of a spherical core consisting of insoluble blocks of polymer B surrounded by a corona of soluble blocks of polymer A swollen by the solvent. Depending on the composition of the starting block copolymers, two limiting structures can be drawn (i) crew-cut micelles with a large core and highly stretched coronal chains (ii) "starlike" micelles with a small core compared to the corona. Micelle properties are the above-mentioned cmc, the aggregation number, the core radius, and the micellar radius. Key parameters that control them are the degree of polymerization of the polymers blocks, N_A and N_B, and the Flory−Huggins parameter χ.[39,40] A large number of studies have been devoted to the scaling of micelle dimensions or properties with copolymer composition using mainly static and dynamic light scatterings.[40] At the same time, several theoretical models have been developed to calculate these micelle properties. In this context, Förster et al. provide a useful table summarizing the scaling relationships from theory for the aggregation number and domain size.[41] In scaling theories, the micellar radius and the aggregation number are directly related to the degree of polymerization of the polymers blocks, N_A and N_B, of the investigated micelles. Among these models, two limiting cases have to be distinguished for the description of the micelle structure: the starlike (or hairy micelles) with $N_A \gg N_B$ and the crew-cut micelles with $N_B \gg N_A$. Daoud and Cotton have developed a scaling model for hairy micelles and have found that the micelle radius is given by the expression $R \propto N_B^{(4)/(25)} N_A^{(3)/(5)}$.[42] Halparin obtained a similar scaling law for a starlike micelle model.[43] For crew-cut micelles ($N_B \gg N_A$), the dependence of the micellar parameters on N_A disappears and one predicts that R increases in proportion to $N_B^{(2)/(3)}$.[44] Thus, the micelle dimensions depend on copolymer composition and in a more general manner, the micelle radius can be expressed as $R \propto N_A^{\alpha} N_B^{\beta}$. α and β values depend on the model and the type of micelles.

In the present work, we propose that the pore radius of mesoporous silica matrices templated with block copolymers can be also expressed as a simple scaling law, i.e., $R_P \propto N_A^{\alpha} N_B^{\beta}$. Although Smarsly et al.[24] also started from this expression to give a quite complicated relationship, we have chosen to maintain a simple relationship taking into account only the block length. Thus in our case, $R_P \propto N_{PEO}^{\alpha} N_{PS}^{\beta}$ and $R_P = C N_{PEO}^{\alpha} N_{PS}^{\beta}$, where C is a constant.

Thus, for both series of mesoporous silica matrices, i.e., for each value of N_{PEO}, the logarithmic variation of the pore radius as a function of N_{PS} was plotted (Figure 4). Indeed, if the pore radius follows the scaling law $R_P = C N_{PEO}^{\alpha} N_{PS}^{\beta}$, the above-mentioned plot should be linear and allow a determination of the β coefficient: $\log(R_P) = \log C + \alpha \log(N_{PEO}) + \beta \log(N_{PS})$.

For each series, i.e., for each value of N_{PEO}, a linear variation of $\log(R_P) = f[\log(N_{PS})]$ is found, suggesting that the power law used allows a description of the evolution of the pore radius as a function of copolymer composition. Furthermore, two parallel straight lines are observed with one corresponding to $N_{PEO} = 232$ above the other ($N_{PEO} = 114$). This means that (i) increasing N_{PEO} leads to an increase of mesopore size, (ii) for both series of samples ($N_{PEO} = 114$ and $N_{PEO} = 232$), the β parameter is the same i.e. the degree of polymerization of the hydrophobic block N_{PS} has the same influence on the pore radius and it is equal to $\beta = 0.5$. Furthermore, as we have two series of experiments, fitting both series of experimental data provides the param-

(39) Gohy, J. F. Block copolymer micelles. In *Block Copolymers II*; Volker, A., Ed.; Advances in Polymer Science Series; Springer: New York, 2005; Vol. 190, p 65.
(40) Xu, R. L.; Winnik, M. A.; Riess, G.; Chu, B.; Croucher, M. D. *Macromolecules* **1992**, *25*, 644.
(41) Forster, S.; Zisenis, M.; Wenz, E.; Antonietti, M. *J. Chem. Phys.* **1996**, *104*, 9956.
(42) Daoud, M.; Cotton, J. P. *J. Phys. (Paris)* **1982**, *43*, 531.
(43) Halperin, A. *Macromolecules* **1987**, *20*, 2943.
(44) Xu, R. L.; Winnik, M. A.; Hallett, F. R.; Riess, G.; Croucher, M. D. *Macromolecules* **1991**, *24*, 87.

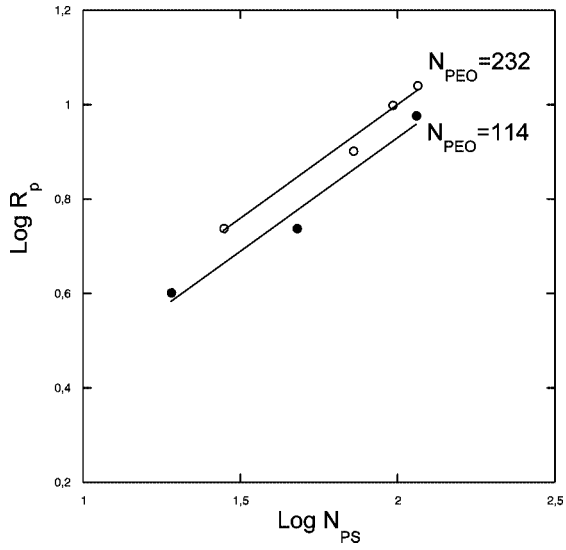

Figure 4. Logarithmic variation of the pore radius as a function of N_{PS} for the two series of silica matrices ($N_{PEO} = 114$ and $N_{PEO} = 232$).

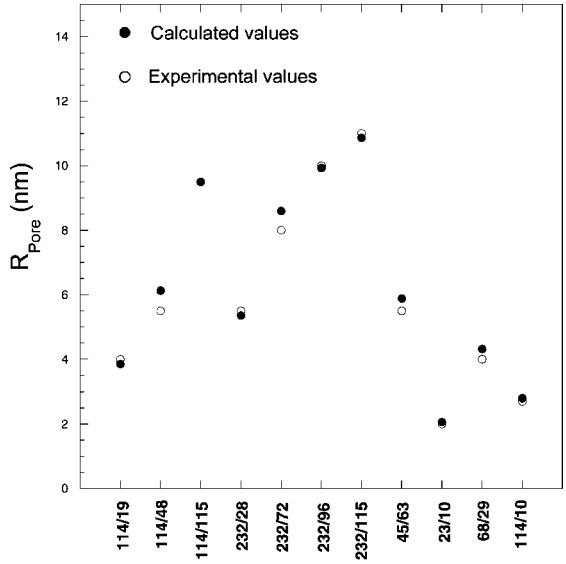

Figure 5. Experimental and calculated values of the pore radius for different mesoporous silicas prepared using PEO-*b*-PS copolymers as templates.

eters $\alpha = 0.19$ and $C = 0.36$ and thus the final power law: $R_P(\text{nm}) = 0.36 N_{PEO}^{0.19} N_{PS}^{0.5}$.

The so-determined power law also highlights the positive contribution of the hydrophilic block (PEO) to the pore radius.

It should be interesting to check the validity of this empirical relationship. With this aim, both calculated and experimental values were plotted on the same graph (Figure 5). Three types of sample were used: (i) the mesoporous silicas which were used to determine this relation, (ii) one mesoporous silica sample prepared in our group (SEO-8 sample from PEO_{45}-*b*-PS_{63} copolymer), (iii) three mesoporous silica samples that were previously studied independently by Göltner and co-workers (from PEO_{23}-*b*-PS_{10}, PEO_{68}-*b*-PS_{29}, and PEO_{114}-*b*-PS_{10} copolymers).[26]

Figure 5 shows that a very good agreement is found for all samples. Thus, this simple empirical relationship allows us to calculate pore dimensions in a large range of pore radius (from 2 to 11 nm). Interestingly, this relationship is valid for both low and high molecular weight copolymers (from 2000 to 22000 g mol^{-1}) and for copolymers presenting a degree of polymerization of the N_{PS} polymer block with $N_{PS} < N_{PEO}$, $N_{PS} \approx N_{PEO}$, and $N_{PS} > N_{PEO}$. Unlike the micellar radius, the mesopore one seems not to depend on the ratio between N_{PS} and N_{PEO}.

This simple power law thus allows us, by choosing the appropriate degrees of polymerization of the PS and PEO blocks, to tune the mesopore radius in a large number of cases.

3.1.4. Evolution of the Microporous Volume. Concerning the evolution of the microporous volume with copolymer composition, it can be seen from Table 2 that the PS block length has an influence on the microporous volume. Indeed, for each series, it is found that increasing the PS block length leads to a diminution of the microporous volume. Working with a constant number of PEO units, we have seen that the mesopore radius (thus the micellar radius) increases with the degree of polymerization N_{PS} and that the contribution of the PEO blocks to the mesoporosity is constant. Thus with increasing N_{PS}, a larger hydrophobic/hydrophilic interface has to be stabilized, leading to a smaller participation of PEO blocks to the microporosity.

It is known that in mesoporous silicas synthesized using either PEO-based AB or ABA copolymers, micropores are generated by the water- and silica-compatible PEO chains. Three scenarios can be envisaged for the structure of the resulting inorganic−organic hybrid material: a three-phase system (inorganic, PEO layer, and hydrophobic core), a two-phase system (PEO inorganic and hydrophobic core), and a transition state between the two- and three-phase models.[15,26] As, in this study, the PEO blocks participate to both the mesoporosity and microporosity, the structure of the inorganic−organic material can be described by this transition state. It is further possible to compare the SEO-3 and SEO-7 samples, where N_{PS} is constant ($N_{PS} = 115$) and N_{PEO} increases. This comparison shows that both the micropore volume and the mesopore size (Table 2) increase with increasing N_{PEO}, confirming the participation of the PEO to both the microporosity and the mesoporosity.

3.2. Influence of the Synthesis Temperature on the Porous Structure. To study the influence of the synthesis temperature on the porous structure two samples were synthesized at different temperatures. Thus, the SEO-3 sample was synthesized at 45 and 60 °C and the SEO-2 sample was synthesized at 60 °C. The synthesis temperature can not exceed 60 °C as the boiling point of tetrahydrofuran is around 65 °C.

The influence of the synthesis temperature on the organization of pores was studied using electronic microscopy and the corresponding TEM pictures are presented in Figures 6a−f.

The sample SEO-2 obtained at 25 °C TEM image (Figure 2b) exhibits an organized porous structure whereas the TEM images obtained for the equivalent sample synthesized at 60 °C (SEO-2-60) shows a disorganized porous network associated with worm like pore geometry. Concerning the sample SEO-3, it can be seen that when the synthesis temperature increases, the porous structure becomes increasingly organized (Figure

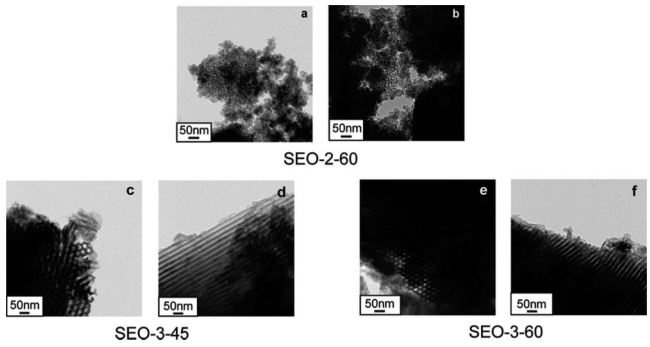

Figure 6. TEM images of calcined mesoporous silicas (a, b) SEO-2 samples synthesized at 60 °C and SEO-3 samples synthesized at (c, d) 45 and (e, f) 60 °C.

Table 3. Porous Properties of the SEO-2 and SEO-3 Samples Synthesized at Different Temperatures

silica samples	D_{pore} (TEM) (nm)	D_{pore} $(BJH)_{ads}$ (nm)	BET area (m^2 g^{-1})	micropore volume (cm^3 g^{-1})
SEO-2	(11 ± 2)	7	421	(0.10 ± 0.01)
SEO-2−60	(7 ± 2)	12	337	(0.06 ± 0.01)
SEO-3	(19 ± 2)	18	239	(0.06 ± 0.01)
SEO-3−45	(20 ± 2)	21	200	(0.05 ± 0.01)
SEO-3−60	(18 ± 2)	21	147	(0.04 ± 0.01)

2c for SEO-3 and Figure 6c−f for SEO-3-45 and SEO-3-60). These results would thus suggest that an optimal temperature is required to the best organization of the structure. Indeed, a certain energy may be required for organization to occur and if this thermal energy is too great then the higher movement of the template leads to disorganization. However, one should also bear in mind that at 60 °C, the synthesis occurs close to the boiling point of THF which may also strongly influence the organization. Indeed, it has been shown that the THF affects the curvature of the micelles.[45] It would seem that the curvature of the micelles is decreased in water−THF mixtures when compared to water only.

These TEM pictures were also used to evaluate the pore diameter of each sample. For samples SEO-3-45 and SEO-3-60, the evaluation of pores diameter was straightforward and the obtained values are reported in Table 3. Nevertheless, the determination of pores diameter for the SEO-2-60 sample was much more difficult as the porous structure is nonorganized with a worm like geometry. Thus, the value reported in Table 3 should be taken only as a prudent estimate.

As can be deduced from the results obtained for sample SEO-3, the synthesis temperature seems not to have an influence on the pore diameter, as differences observed are in the error range.

Nitrogen sorption measurements were also performed in order to investigate the structural properties of theses samples (pore diameter, BET surface area, microporous volume, etc.). The nitrogen adsorption−desorption isotherms obtained for samples SEO-2 and SEO-3 synthesized at different temperatures are shown in panels a and b in Figure 7. The corresponding structural parameters calculated from these isotherms are listed in Table 3. All isotherms are again characteristic of both type I and type IV, representative of microporous and mesoporous solids. In the case of the SEO-2 sample, there is a large change in isotherm form that can easily be related to the change in pore structure from an organized, cubic system (at 25 °C) to a more disorganized wormhole like system (60 °C). The isotherms show a shift in the position of both adsorption and desorption branches indicating an increase in pore size (see Table 3).

Concerning SEO-3, a first observation can be made that concerns the adsorption branch, which remains mainly unchanged by the increase of the synthesis temperature; this means that the mesopore size is practically not or only slightly affected (Table 3). One can see that the mesopore sizes determined by the BJH method are in fairly good agreement with those determined by TEM measurements. The main difference observed in all isotherms with the increase in synthesis temperature lies in the desorption branch. As can be seen from Figure 7b, when the synthesis is carried out 60 °C, the desorption branch occurs at higher relative pressure compared to the one prepared at 25 °C. One can note that for sample SEO-3-60, the desorption branch only overlaps to the adsorption one at $p/p^0 = 0.45$. An intermediate behavior is found for the SEO-3-45 sample. Indeed, it presents a desorption branch occurring in two steps: a first step at $p/p^0 = 0.85$ and a second one at $p/p^0 = 0.45$. As mentioned previously, the desorption branch found at $p/p^0 = 0.45$ is typically observed for mesopores presenting samples entrances estimated to 3−4 nm using the BJH method.[35] Thus, the shift in the desorption band observed for samples prepared at 45 and 60 °C indicates an important increase of the pore entrances sizes. For sample SEO-3−45, two pore entrance sizes are found that are estimated using the BJH method of around 15 nm and 3−4 nm. Finally, it can be noted that the empirical relationship demonstrated above for a synthesis temperature of 25 °C also holds for the synthesis performed at 45 and 60 °C.

When looking to the literature in some cases, it has been shown that when the synthesis temperature increases, the pore entrance size increases, leading to a more open porous structure, whereas the mesopore diameter remains mostly constant. Looking at the literature, Matos et al.[46] have found for FDU-1 silica samples prepared using a PEO-based triblock copolymers that the increase in the synthesis temperature (from room temperature to 80 °C) leads to a change in the shape of the desorption branch isotherm for samples prepared at high temperature ($T = 80$ °C). This phenomenon was also interpreted in terms a modification of pore entrance sizes. They also found that the mesopores diameter increases with the synthesis temperature in an important manner (around 30%).

Nevertheless, a general trend concerning this increase of mesopore diameter with synthesis temperature cannot be found in the literature. Indeed, Kleitz et al.[17] have found in the case of KIT-5 (large mesopores silicas prepared using F127) that an increase of the synthesis temperature from 45 to 100 °C leads to an increase in mesopore size of about 30−40%. Galarneau

(45) Kirmayer, S.; Dovgolevsky, E.; Kalina, M.; Lakin, E.; Cadars, S.; Epping, J. D.; Fernandez-Arteaga, A.; Rodriguez-Abreu, C.; Chmelka, B. F.; Frey, G. L. *Chem. Mater.* **2008**, *20*, 3745.

(46) Matos, J. R.; Kruk, M.; Mercuri, L. P.; Jaroniec, M.; Zhao, L.; Kamiyama, T.; Terasaki, O.; Pinnavaia, T. J.; Liu, Y. *J. Am. Chem. Soc.* **2003**, *125*, 821.

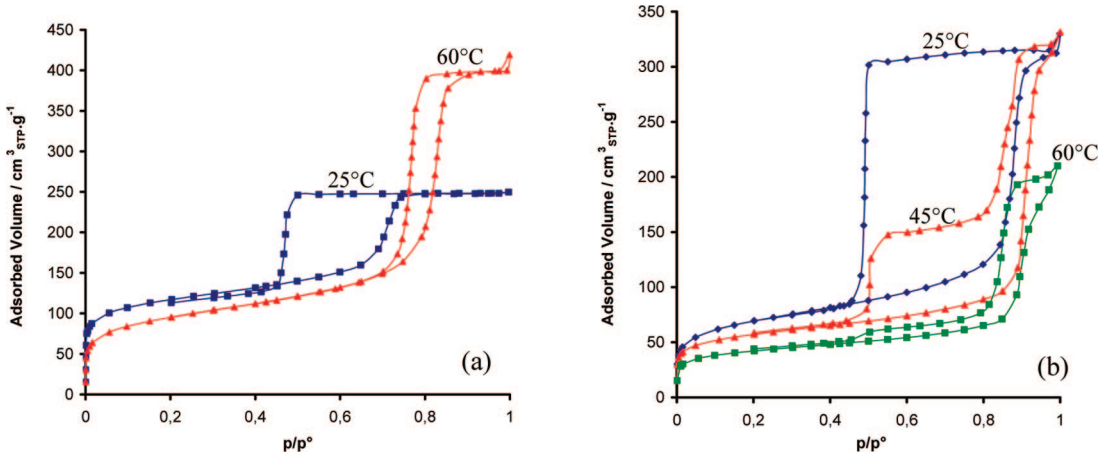

Figure 7. Nitrogen adsorption/desorption isotherms of (a) SEO-2 samples synthesized at 25 and 60 °C, and (b) SEO-3 samples synthesized at 25, 45, and 60 °C.

et al.[47] have demonstrated using platinum replicas of the porous structure of SBA-15 samples, that an increase in the synthesis temperature (from 35 to 130 °C) leads to first a constant mesopore diameter (until $T = 60$ °C) and then to an important increase of mesopore size (around 50%) for temperatures above 60 °C. In another study, Van der Voort et al.[48] have shown in the case of SBA-16 samples, that an increase of the synthesis temperature from 25 to 65 °C does not lead to an increase of the mesopore diameter. As the synthesis conditions are not the same, it is difficult to compare all these data between them and with ours. Nevertheless, the increase in the mesopore diameter with increasing synthesis temperature, in the case of silicas prepared using PEO-based copolymers, is generally explained by considering that the hydrophobicity of the PEO blocks increases with the temperature. As the hydrophobicity of the PEO blocks increases, their degree of hydration decreases dramatically at high temperatures, leading to their transfer into the hydrophobic core of the micelle. This results in an increase in the micelle core size and, thus, in the subsequent mesopore diameter.[48] In our case, as the synthesis temperature cannot exceed 60 °C because of the boiling point of THF, one can consider that the hydrophobicity of PEO blocks is not sufficiently changed to strongly affect the micelle core size and thus the mesopore one. This interpretation is reinforced by the evolution of the microporous volume as a function of the synthesis temperature. Indeed, the microporous volume decreases with increasing the synthesis temperature of about 40% for SEO-2−60 sample and of about 20% for SEO-3-60). One can consider that there are still some PEO blocks penetrating the silica walls and thus, that the hydrophocity of these PEO blocks is not strongly increased.

4. Conclusion

In this study concerning the synthesis of large pore mesoporous silicas using PEO-*b*-PS diblock copolymer templates, the first aim was to understand the role of each block on the porosity formed. With this in mind, a number of diblock copolymers were prepared using the simple nitroxide mediated polymerization method. Two series of silica samples were prepared with templates presenting two different degrees of polymerization of the PEO block, N_{PEO}. The general trends show that an increase in the degree of polymerization of the PS block, N_{PS}, leads to a decrease in pore organization, an increase in mesopore size and a decrease in micropore volume. Furthermore, although the PS block only participates to the mesoporosity, the PEO block participates to both the microporosity and the mesoporosity. Finally, the small pore materials seem to organize in the $Pm\bar{3}m$ symmetry, which is lost for the larger pore systems.

This work has allowed a simple empirical relationship to be proposed that is based on that found for diblock copolymer micelle formation in solution. This relationship has been verified against a further sample made in the framework of this study and with others previously documented in the open literature. This relationship seems to hold for a large variation in degrees of polymerization of PS block compared to PEO one. It can thus be used to prepare silica materials with pore diameter from few nanometers to more than 20 nm. This therefore opens the possibility, for the first time, to predict and fine-tune large pore mesoporous materials for specific applications.

The second aim of this study was to investigate the influence of the synthesis temperature on the porous structure. While the effect of the synthesis temperature on the porous structure is quite difficult to understand, this work shows that an increase in the synthesis temperature leads to an increase in the pore entrances size and thus to a more open porous structure. Furthermore, the synthesis temperature seems not to have an influence on the mesopore size even though the pore organization varies. Finally, it highlights the differing behavior dependence on the given copolymer used as template.

Acknowledgment. The authors acknowledge the EU STREP project 'DeSANNS' (SES6-CT-2005-020133) for financial support and ARKEMA for the kind provision of BlocBuilder (MAMA-SG_1) products. The authors also gratefully acknowledge P. Davidson, M. Impéror, D. Constantin, and C. Rochas for the SAXS measurements, as well as W. Saikaly for the TEM images.

CM801978W

(47) Galarneau, A.; Cambon, N.; Di Renzo, F.; Ryoo, R.; Choi, M.; Fajula, F. *New J. Chem.* **2003**, *27*, 73.

(48) Van der Voort, P.; Benjelloun, M.; Vansant, E. F. *J. Phys. Chem. B* **2002**, *106*, 9027.